JOURNAL OF CATALYSIS 113, 236–249 (1988)

Surface and Bulk Changes in Iron Nitride Catalysts in H_2/CO Mixtures

A. A. HUMMEL,[1] A. P. WILSON,[2] AND W. N. DELGASS

School of Chemical Engineering, Purdue University, West Lafayette, Indiana 47907

Received February 16, 1988; revised April 19, 1988

Preparation of the ζ-, ε-, and γ'-iron nitride phases was confirmed by Mössbauer spectroscopy, X-ray diffraction, and quantitative mass spectrometry of NH_3 evolved during decomposition. Computer fitting of the ε-nitride Mössbauer spectra with a distribution of hyperfine fields shows the conversion of iron with two nitrogen nearest neighbors (Fe 2nn) to Fe 3nn as the nitrogen content increases. The dynamic response of the nitrides to H_2/CO mixtures at reaction temperatures was followed by constant-velocity Mössbauer spectroscopy and transient mass spectrometry. The rapid decomposition of the iron nitrides in H_2 at 523 K occurs with surface reaction as the rate limiting step, initially. At lower temperatures or after significant nitride decomposition, the data are best fit with a shrinking core model. For reaction at 473 K, the Mössbauer effect identified an α-Fe shell, a ζ-Fe_2N core, and an ε-Fe_xN transition region. Surprisingly, loss of the pure nitride phase is barely retarded for H_2/CO mixtures compared to H_2 alone at 523 K. Mass spectrometric studies show that the freshly prepared nitride has a substantial hydrogen inventory, equivalent to a monolayer of NH_3 for ζ-Fe_2N. On exposure to synthesis gas, the nitride catalysts produce no methane until one to two monolayers of N have been removed, but carbon is deposited on the catalyst by the Boudouard reaction. Mass spectral measurements show no evidence for active nitrogen on the surface after the synthesis reaction has been established. Both Mössbauer spectroscopy and mass spectral measurements confirm, however, that following the initial loss of nitrogen, bulk carbonitrides form which lose their nitrogen very slowly as the reaction proceeds. These data suggest that differences in the performance of iron and iron nitride catalysts may be strongly influenced by the way surface carbon is deposited during reactor startup.

INTRODUCTION

Iron nitride Fischer–Tropsch catalysts have been found by Anderson and co-workers at the Bureau of Mines (*1–3*) to provide higher activity, long life, somewhat shorter product chain lengths, and significantly higher alcohol production rates than promoted fused iron catalysts. Studies by Yeh *et al.* (*4, 5*) indicate somewhat different selectivities at lower conversion but confirm the higher activities for a promoted catalyst at 7.8 and 14 atm pressure for a 1 : 1 H_2 : CO mixture. Most significant in both studies, however, is the extremely long life of bulk nitrogen during exposure to H_2/CO mixtures, whereas in pure H_2 nitrided catalysts are extremely unstable. The stability of these catalysts in various gas-phase atmospheres is, therefore, a central issue in their performance. In this paper, we examine the preparation and stability of the different unsupported nitride phases, γ'-Fe_4N, ε-Fe_xN ($2 < x < 3$), and ζ-Fe_2N as Fischer–Tropsch catalysts.

Preparation of the three major phases of iron nitride can be accomplished by varying the NH_3/H_2 nitriding compositions and/or temperature, as reported by numerous authors (*1, 6–8*). The different nitride stoichiometries are easily identified by their characteristic Mössbauer spectra (*4, 9*). Stoichiometries and phase identification can also be confirmed by X-ray diffraction

[1] Present address: Technisch-Chemisches Laboratorium, ETH-Zentrum, CH-8092 Zürich, Switzerland.

[2] Present address: Arco Oil and Gas, Plano, TX 75074.

0021-9517/88 $3.00

(*7*) and mass spectrometric measurement of the ammonia evolved during decomposition in hydrogen.

In this work, both steady-state and dynamic Mössbauer results indicate that the pure nitride phases are highly unstable in both hydrogen and synthesis gas. The bulk nitrides are completely lost to ammonia and α-Fe in hydrogen, whereas they form stable carbonitrides in synthesis gas. Results from transient mass spectrometric investigation of the surface chemistry during the hydrocarbon synthesis reaction illustrate an important factor in the stability of nitrogen in the steady-state carbonitride form of these catalysts. They suggest that carbon, resulting from the dissociation of carbon monoxide, effectively blocks the surface sites necessary for hydrogenation of bulk nitrogen. Apparently, no active surface nitrogen is present during Fischer–Tropsch synthesis.

EXPERIMENTAL

The unsupported iron oxide catalyst precursors used for this study were prepared by precipitation of iron hydroxide from a mixture of NH_4OH and a 0.17 *M* $Fe(NO_3)_3$ solution. The filter cake was dried in air at 370 K, pulverized, and then oxidized at 573 K to form Fe_2O_3. For a second batch of catalyst prepared for the Mössbauer studies, the oxidation was carried out at 500 K. For the Mössbauer experiments, 25 mg of iron oxide precursor and 200 mg of Cab-O-Sil EH-5 silica, mixed in as a diluent, were mechanically pressed into a self-supporting 1.5-cm-diameter wafer, approximately 1.5–2.0 mm in thickness. For the transient mass spectrometry experiments, 100 mg of precursor was packed between Pyrex wool plugs in a 6-mm-o.d. Pyrex reactor tube. Individual samples of catalyst precursor were reduced in flowing H_2 for at least 4 h at 673 K before nitriding. The surface area of the reduced catalysts was determined by flowing BET measurements (*10*). The catalyst used for the Mössbauer experiments, without the silica diluent, gave a nitrogen uptake at 77 K corresponding to a surface area of 1.6 ± 0.1 m^2/g of reduced Fe. The samples calcined at 573 K and used for transient mass spectrometry had a surface area of 4.3 ± 0.1 m^2/g.

Both constant-acceleration and constant-velocity *in situ* Mössbauer spectra were obtained with an Austin Science S-600 spectrometer controller. Data were acquired in 256 channels of a Nuclear Data Model 62 multichannel analyzer. The 70-mCi gamma ray source, ^{57}Co diffused into a Rh matrix, was obtained from New England Nuclear. Zero isomer shift was referenced to the center of a 25-μm NBS Fe foil spectrum. Room-temperature spectra were obtained after the sample had cooled to ambient temperature in the appropriate gas mixture. The stability of the individual nitride phases was investigated under reaction conditions using the constant-velocity (transient) mode which monitors the count rate at a particular velocity rather than scanning over all velocities as in the more familiar constant-acceleration mode (*11*).

The constant-acceleration spectra were computer fit with a routine developed by Niemantsverdriet (*12, 13*) and modified by Gregg Howsmon of our laboratory. The program fits optionally fixed or variable isomer shift, quadrupole splitting, hyperfine field, and linewidth for each spectral species. The individual spectral lines corresponding to each species are calculated from component parameters so that they conform to the physics of the Mössbauer effect. The program employs a Levenberg–Marquardt nonlinear regression formula to converge on the least-squares optimum fit. In addition, the program contains a computational procedure for evaluation of the probability density of a distribution of hyperfine fields (*14, 15*). A distribution may be fit independently or in conjunction with additional singlet, doublet, or six-line components.

The transient kinetic apparatus consists of a glass tube reactor within brass sheathing heated by a Research Incorporated IR oven and controlled by a Micristar tem-

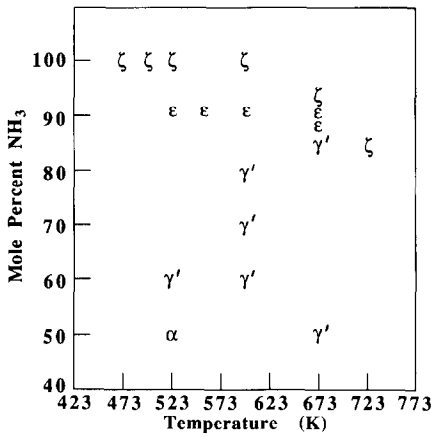

FIG. 1. Temperature and percentage NH_3 in H_2 required to form the nitride phases indicated in 3–4 h. α = Fe, γ' = Fe_4N, ε = Fe_xN ($2 < x < 3$), ζ = Fe_2N.

perature controller. The reactor can be fed with gas from any of three manifolds or a pulse loop for introduction of isotopically labeled components. Products, or reactants passed through a reactor bypass, are analyzed by an Extrel Corp. EMBA II modulated beam quadrupole mass spectrometer interfaced to a Digital Equipment Corp. MINC-11 minicomputer for data acquisition. The modulated beam design allows for detection of inlet components and discrimination against background gases within the mass spectrometer chamber and gives significant improvement in transient monitoring of strongly absorbing gases such as NH_3 or H_2O.

X-ray diffraction (XRD) was performed on a Siemens Kristalloflex 4 spectrometer using Cu$K\alpha$ X-rays. The three major nitride phases are easily differentiated via their unique diffraction patterns.

All gases used for these experiments were Matheson UHP grade. Molecular sieve and Scott oxygen traps further purified helium and hydrogen. Metal carbonyls in CO were removed in a molecular sieve trap at dry ice-methanol temperature (216 K).

RESULTS AND DISCUSSION

Preparation of the individual bulk nitride phases can be accomplished at atmospheric pressure in different NH_3/H_2 mixtures and at different temperatures. Figure 1 shows the conditions necessary to produce each of the phases after 3–4 h of nitriding. Our results are in general agreement with those of Lehrer (*6*) and Bouchard *et al.* (*8*). Both the ζ-Fe_2N (or, in some cases, ε-Fe_xN with $2 < x < 2.1$) and the γ'-Fe_4N phases are easily formed over a variety of temperatures and ammonia/hydrogen gas-phase compositions, whereas the ε-Fe_xN ($2.1 < x < 3$) phase is produced only in a narrow composition range (90 ± 5% NH_3).

Characterization of each of the pure phases was accomplished by Mössbauer spectroscopy and, for a few specific samples, by X-ray diffraction. Figure 2 shows the room-temperature Mössbauer spectra of the different nitrides. The solid lines in the spectra are the result of careful

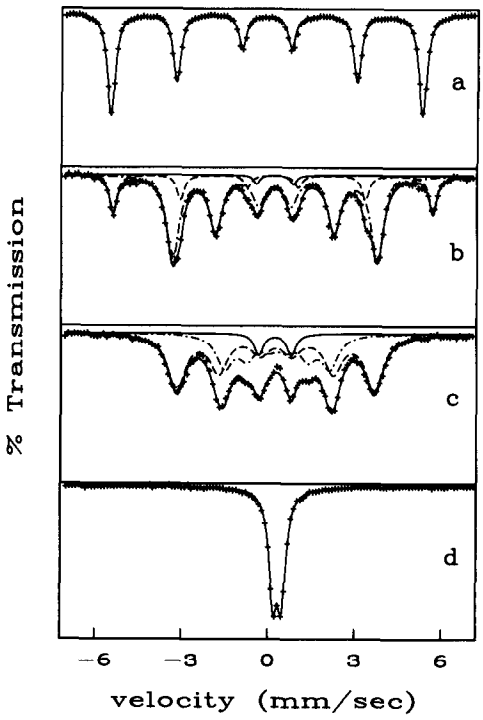

FIG. 2. Room-temperature Mössbauer spectra of iron and the single-phase nitrides. (a) α-Fe, (b) γ'-Fe_4N, (c) ε-$Fe_{2.52}N$, (d) ζ-Fe_2N. The interior subspectra are for the iron species used in curve fitting (see Table 1).

TABLE 1

Room-Temperature Mössbauer Parameters for Single-Phase Nitrides in Fig. 2

Figure	Species	I.S. (mm/s)	Q.S. (mm/s)	H (kOe)	Width (mm/s)	% area
2a	α-Fe	0.0	0.00	330.7	0.33	100
2b	γ'-Fe_4N					
	Fe-I	0.23	0.00	339.5	0.32	21.4
	Fe-II	0.30	0.00	217.4	0.52	76.3
	Fe-Q	0.30	1.26	—	0.27	2.2
2c	ε-$Fe_{2.52}N$					
	Fe-II	0.34	−0.01	210.1	0.73	60.6
	Fe-III	0.40	0.00	111.8	0.68	33.2
	Fe-Q	0.32	1.11	—	0.38	6.2
2d	ζ-Fe_2N	0.44	0.29	—	0.35	100

computer fitting, with parameters summarized in Table 1. In these fits, all the values of linewidth, isomer shift, quadrupole splitting and hyperfine field for a given iron species are fitted and not independently fixed. XRD of the separate phases distinguished among the fcc, hcp, and orthorhombic structures of the γ', ε, and ζ phases, respectively, confirming the synthesis of a ζ-Fe_2N sample from 100% NH_3 at 673 K, an ε phase from 85% NH_3 at 673 K, and a γ' phase from 75% NH_3 at 598 K (*7*).

The γ'-nitride (Fig. 2b) is identified by a characteristic eight-line pattern arising from a partial overlap of the hyperfine fields of Fe-I atoms, which occupy the corner sites and have no nitrogen nearest neighbors (0nn) and Fe-II atoms, which are at the face-centered sites and have two nitrogen nearest neighbors (2nn). The most positive velocity peak (5.71 mm/s), which is the outermost peak of the 340-kOe field lines corresponding to Fe-I, does not overlap with either iron or the other nitrides and serves to indicate the presence of γ'-Fe_4N in complex, multiphase spectra. The γ'-nitride can also be fit with three different sextets (Fe-I, Fe-IIA, and Fe-IIB), as demonstrated by Clauser (*16*) and Nozik *et al.* (*17, 18*). The Fe-IIA and Fe-IIB sextets both have the same hyperfine field and small, but different, quadrupole shifts. The γ'-Fe_4N spectra shown in this work were not of sufficient resolution to resolve the Fe-IIA and Fe-IIB sites.

The fitting of Fig. 2b was done with two sextets and a small central doublet, as reported in Table 1. The Fe-Q doublet, necessary to achieve a close fit, appears in all the fits of the nitrides and usually has a small area (with the exception of certain ε-nitrides). This component may arise from the existence of a paramagnetic phase (Fe-III), amorphous Fe^{3+} (*4*), or alternatively, microcrystals, of an iron phase contained within a larger particle (*19*). This last case is best described by relaxation phenomena (*20*) resulting when the particle volume is so small that its magnetization vector is no longer fixed in space over the Larmor precession time of the nucleus (*21*). In Table 1, we have neglected any distributions of hyperfine fields that may exist for one particular iron site. This complication will be considered in the discussion of the ε nitrides.

Spectra of the hexagonal close-packed nitrides, ε-Fe_xN ($2 < x < 3$), are shown in Figs. 2c and 3. The spectra in Fig. 3 repre-

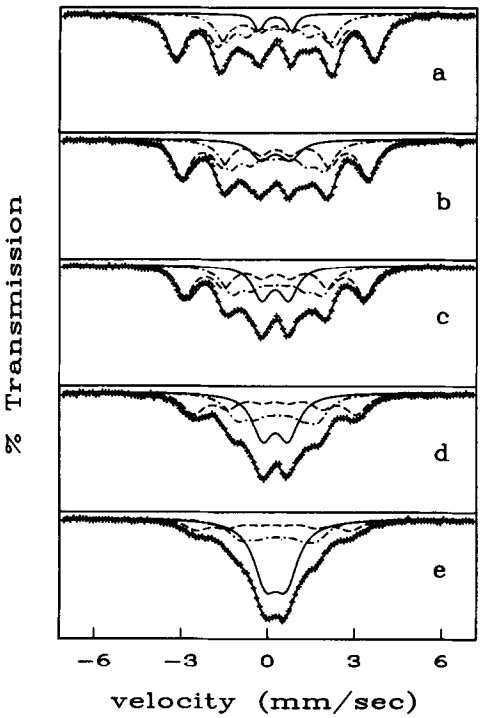

FIG. 3. Room-temperature Mössbauer spectra of ε-Fe_xN prepared by 6-h exposure under the conditions listed. (a) $Fe_{2.52}N$, nitrided in 90% NH_3 at 598 K; (b) $Fe_{2.39}N$, nitrided in 91% NH_3 at 523 K, (c) $Fe_{2.33}N$, nitrided in 91% NH_3 at 553 K, (d) $Fe_{2.25}N$, nitrided in 91% NH_3 at 598 K, (e) $Fe_{2.14}N$, nitrided in 91% NH_3 at 673 K. The interior subspectra are for Fe (2nn), Fe (3nn), and Fe-Q (see Table 2).

sent a range of stoichiometries presented from top to bottom in order of increasing nitrogen content. As the stoichiometry approaches Fe_2N, the magnetic field collapses to form a broad doublet (Fig. 3e). Spectra of the ε-nitride can be fit with a combination of 3nn and 2nn sites (Table 2), such that $H_{3nn} < H_{2nn}$, and an additional nonmagnetic, quadrupole split component, Fe-Q. An increase in covalent bonding character and a decrease in Curie temperature, T_c, occur as the composition changes from Fe_3N to Fe_2N (*9*). Therefore, as the nitrogen content increases, the magnetic moment and hyperfine field measured at room temperature decrease. Note that the Fe-Q component increases from 6% of the spectral area (Fig. 3a) to 50% (Fig. 3e) as the nitrogen content increases, and thus behaves as a paramagnetic 3nn site that approaches the iron environment of the ζ-nitride. Yeh *et al.* have accurately assigned a wide doublet (with QS > 1) to amorphous Fe^{3+} (*4*). The increasing amount of Fe-Q with increasing NH_3 partial pressure in our experiments, however, indicates that Fe-Q should be assigned to Fe(3nn) in ε-nitride in this case.

The average stoichiometry of the ε-nitrides is estimated from the spectral areas of each of the three components, assuming equal recoil free fractions and three nitrogen nearest neighbors for the Fe-Q composition (*22*). The composition range in Fig. 3 is then from $Fe_{2.52}N$ to $Fe_{2.14}N$, as indicated in Table 2.

In these fits, we have assumed that the electric field gradient and hyperfine field are unique for a particular iron site. However, the environment of an iron nucleus in a particular ε-nitride site may vary as a result of the wide range of stoichiometries and configurations of nearest and next nearest neighbor nitrogen placements possible for this phase (*9, 23*). Accordingly, a distribution of hyperfine fields is expected from the random distribution of nitrogen surrounding each iron site. One method of approximating this distribution is given by Chen *et al.* (*9*) and Yeh *et al.* (*4*) who have used sextets with linewidths that are an increasing function of velocity to fit iron nitride spectra. A sextet with a slightly different hyperfine field but the same isomer shift would overlap a given six-line spectrum most at velocities close to zero and overlap least for the outer peaks. Thus, when the components are combined, the spectral envelope shows peaks with greater linewidths as the absolute value of the velocity increases.

Alternatively, distributions of hyperfine field can be fit directly with a distribution of discrete hyperfine fields equally spaced over the hyperfine field range (*14, 15*). The method includes a parameter for smoothing the distribution and zero factors at the

TABLE 2

Room-Temperature Mössbauer Parameters for ε-Fe_xN in Fig. 3

Figure	Species	I.S. (mm/s)	Q.S. (mm/s)	H (kOe)	Width (mm/s)	% area
3a	ε-$Fe_{2.52}N$					
	Fe-II	0.34	−0.01	210.1	0.73	60.6
	Fe-III	0.40	0.00	111.8	0.68	33.2
	Fe-Q	0.32	1.11		0.38	6.2
3b	ε-$Fe_{2.39}N$					
	Fe-II	0.34	−0.01	196.7	0.69	48.1
	Fe-III	0.43	−0.02	101.1	0.75	37.2
	Fe-Q	0.35	1.01		0.82	14.7
3c	ε-$Fe_{2.33}N$					
	Fe-II	0.34	−0.01	190.2	0.70	41.0
	Fe-III	0.42	−0.01	96.3	0.80	36.7
	Fe-Q	0.33	0.92		0.73	22.2
3d	ε-$Fe_{2.25}N$					
	Fe-II	0.34	−0.01	172.3	0.87	32.1
	Fe-III	0.45	−0.03	85.7	0.89	35.2
	Fe-Q	0.36	0.87		0.84	32.7
3e	ε-$Fe_{2.14}N$					
	Fe-II	0.26	0.03	162.7	0.98	20.3
	Fe-III	0.48	−0.03	81.8	0.97	28.6
	Fe-Q	0.37	0.69		0.96	51.1

endpoints to avoid physically unrealistic fluctuations in the distribution. We have fit the series of ε-nitrides with distributions over the entire hyperfine field range and show the distributions in Fig. 4. Since the program uses the same quadrupole splitting and isomer shift for the entire distribution, the results are approximate. Nevertheless, Fig. 4 graphically demonstrates the two separate fields and the decay of the amount of the high hyperfine field species and the corresponding growth of the lower hyperfine field species as nitrogen content increases. Note also the increasing density near zero field. This represents the growth of the wide Fe-Q doublet, which may be due to the onset of paramagnetism at room temperature for iron sites with three nitrogen nearest neighbors. This effect is only markedly significant in the highest nitrogen concentration ε-nitride. We note that the field is collapsing as the Neél temperature of the ε-nitrides nears room temperature (*23*), a phenomenon that has been simulated for iron carbides empirically by Lin and Phillips (*24*). The distribution fit is, therefore, only an approximation of the physics in this case.

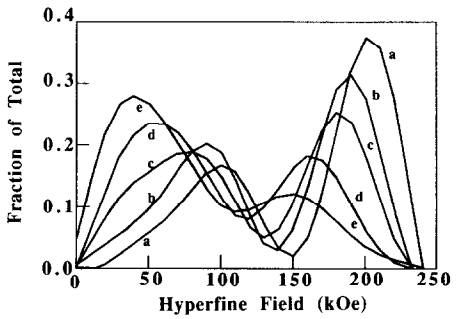

FIG. 4. ε-Fe_xN Mössbauer fits using a distribution of hyperfine fields. The letter next to each curve indicates the spectrum in Fig. 3.

The last nitride considered is the nitrogen-rich phase, ζ-Fe_2N. This orthorhombic, nonmagnetic phase is characterized by a central doublet, as shown in Figs. 2d and 5b. In this phase, all iron atoms have three nitrogen nearest neighbors. The spectrum does not split out even at 4.2 K (*25*). The room-temperature spectrum, Fig. 2d, has an isomer shift of 0.43 mm/s and a quadrupole splitting of 0.28 mm/s. Similar spectra displayed by Chen *et al.* (*9*) and Yeh *et al.* (*4*) for ε-Fe_xN indicate that the onset of paramagnetism at room temperature occurs approximately at ε-Fe_xN with $x < 2.2$ and results in a sharp doublet indistinguishable from the ζ-nitride spectrum at room temperature. The phase assignment for the ζ-nitride has been confirmed, however, by XRD.

Iron Nitride Stability

The collection of a Mössbauer spectrum can take between 4 and 24 h depending on the strength of the source and the amount of ^{57}Fe in the sample. The usual constant acceleration mode of data accumulation is, therefore, much too slow for transient experiments. If, however, one measures the count rate at a carefully chosen single velocity, one can follow spectral changes on a time scale of minutes (*11*). Application of this technique to the denitriding and renitriding of ζ-Fe_2N is shown in Fig. 5. Choice of the constant velocity point at the minimum in the ζ-nitride doublet, spectrum 5b, allows good sensitivity to changes in the amount of the nitride phase because this happens to be a region of the iron metal spectrum (Fig. 5c) where the transmission is nearly 100% (no peak). Curve 5a shows the loss of ζ-nitride (rise in transmission) in hydrogen and growth of the ζ-nitride in ammonia and indicates very fast removal of nitrogen in the presence of pure hydrogen. In a matter of minutes, Fe_2N has become iron metal, as confirmed in spectrum 5c. Renitriding is slower because the nitrogen must penetrate the hexagonal close-packed nitride lattice rather than the more open bcc

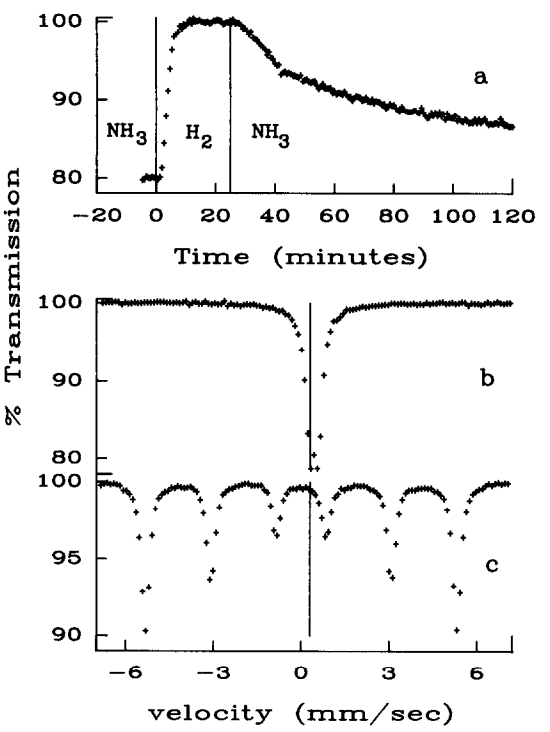

FIG. 5. *In situ* analysis of ζ-Fe_2N denitriding in H_2 and nitriding in NH_3 at 523 K. (a) Constant-velocity Mössbauer spectrum of denitriding and nitriding at the velocity indicated in the constant-acceleration spectra for ζ-Fe_2N (b) and α-Fe (c), obtained after a 5-min H_2 reduction of ζ-Fe_2N.

structure of α-Fe. The rapid nitride loss shown in Fig. 5a is not surprising since the nitrides are known to be unstable in hydrogen (*1–3, 25–27*).

Figure 6 displays the constant-velocity spectra that indicate the stability of the pure ζ-nitride phase in different atmospheres at 523 K. Figure 6a, which shows the denitriding process in pure hydrogen, reproduces the results of Fig. 5 and contrasts with the extremely slow rate of denitriding observed in a helium atmosphere (Fig. 6c). Surprisingly, comparison of Figs. 6b and 6a shows that the time required for complete loss of the ζ-Fe_2N phase is barely retarded by the change from hydrogen to synthesis gas at 523 K. In this case, however, constant-acceleration spectra after varying times of exposure show that

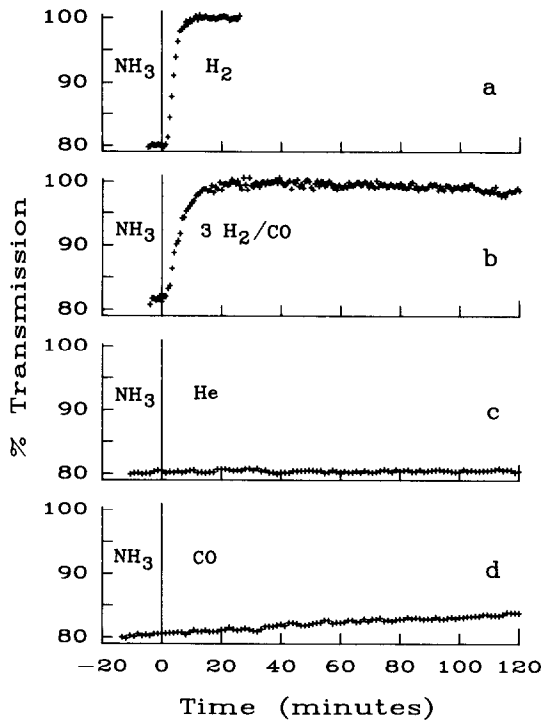

FIG. 6. Constant-velocity analysis of ζ-Fe_2N denitriding at 523 K in the gas atmospheres indicated.

the nitride is not converted into the metal, but first, as also reported by Chen *et al.* (*9*), into the ε-nitride (see Fig. 11) and then into a carbonitride. In pure hydrogen at 523 K, therefore, nitrogen is completely lost to the gas phase, whereas much of the nitrogen remains in the bulk after the nitrides are exposed to synthesis gas. Figure 5d shows that the rate at which the pure nitride phase is lost can be slowed significantly if all the hydrogen is removed from the synthesis gas.

We have studied the nitrogen removal process in some detail. Using computer-controlled transient mass spectrometry, we have monitored the decomposition products in the effluent of a differential plug flow reactor as a function of time. Heating an iron nitride sample in flowing helium and monitoring the gas-phase effluent for N_2 produces a temperature-programmed decomposition spectrum of the nitride. Such experiments confirm the Mössbauer findings that at temperatures below 600 K, the nitrides are stable in helium. When a freshly prepared nitride is flushed with a short pulse of He to remove the NH_3/H_2 synthesis mixture and then exposed to H_2 at 523 K, the ammonia concentration in the effluent is a measure of the nitride decomposition rate. Figure 7 displays the results of two separate experiments, the decomposition of an ε-$Fe_{2.7}N$ nitride and of a γ'-Fe_4N nitride in H_2 at 523 K. The complete removal of nitrogen after about 5 min is consistent with the instability of the nitrides in hydrogen as already discussed. The area under the NH_3 curve represents the total amount of nitrogen in the nitride. The stoichiometries predicted by this measurement are $Fe_{2.7}N$ and $Fe_{3.9}N$ for the ε- and γ'-nitride decompositions respectively, which are correct for these phases within the uncertainty of the integration (10%).

The fact that the curves in Fig. 7 slowly rise to a maximum rather than decaying from a maximum at the initial contact with hydrogen has been reported in the literature previously (*27*). This behavior shows clearly that nitrogen removal at these temperatures is not simply a diffusion-limited process, which would have a maximum rate at the beginning when the transfer area is a maximum and the diffusion distance is a minimum. One model that can account for this phenomenon is a reaction sequence that includes competition for surface sites between adsorbed hydrogen and surface

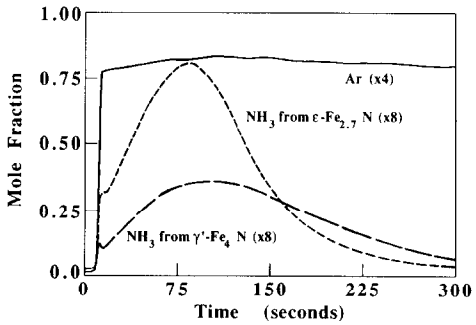

FIG. 7. Transient mass spectrometric measurements of the decomposition of iron nitrides in 4 : 1 H_2 : Ar at 523 K. The Ar trace is for the γ'-Fe_4N experiment.

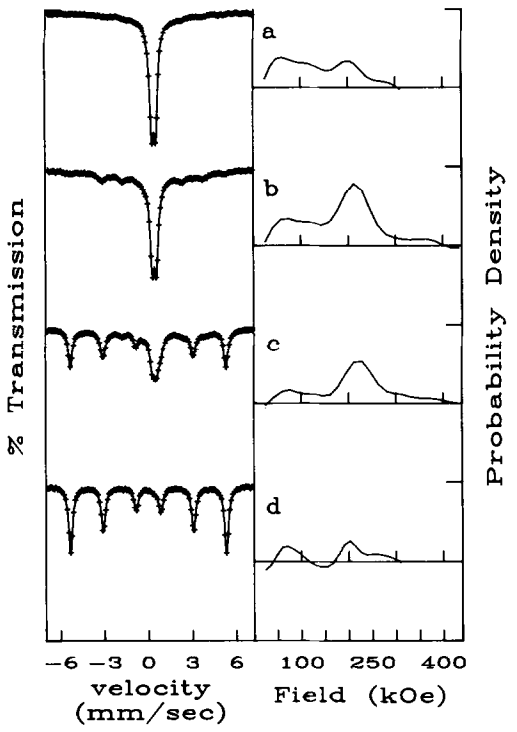

FIG. 8. Room-temperature Mössbauer spectra of quenched intermediate samples during the decomposition of ζ-Fe_2N in H_2 at 473 K. The curves to the right of each spectrum are the distribution fits of the residual spectra after subtracting the ζ-Fe_2N and α-Fe fractions. (a) After 2.5 min of H_2, (b) after 5 min, (c) after 10 min, (d) after 21 min.

nitrogen that diffuses from the bulk. Fast conversion of bulk nitrogen to surface nitrogen species initially limits the amount of surface hydrogen and restricts the rate. As decomposition proceeds, the N arrival rate at the surface is slowed, and surface hydrogen coverage increases allowing the rate to build to a maximum. On the right side of the maximum, the rate is limited by the concentration of surface nitrogen, a consequence of the decreasing amounts of bulk nitrogen and diffusion-limited transport.

At lower temperatures (473 K), diffusion through the bulk is rate limiting, and the separate phases can be distinguished during the denitriding. A "shrinking nitride core" picture is confirmed by the Mössbauer spectra in Fig. 8, which show a discrete transition from ζ-Fe_2N to α-Fe as monitored at intermediate points in the denitriding. To obtain these data, the temperature of the catalyst wafer and the surrounding Mössbauer cell was quenched to room temperature by pouring liquid nitrogen onto the top of the heater block. The sharp doublet in the spectrum of Fig. 8a is indicative of ζ-Fe_2N, whereas the six-line pattern in Fig. 8d is α-Fe. The fitted contribution from ε-nitrides, which represent the gradient between the ζ core and the α-Fe outer shell, is best represented by the hyperfine field distributions shown on the right-hand side of the figure. The total area of the ε-nitrides in each spectrum ranges from 8% (Fig. 8d) to 43% (Fig. 8b) and is reflected in the scaling of the y-axis of the distribution curves. The fitted parameters are given in Table 3.

The distribution of ε-nitrides (and perhaps a trace of γ'-nitride in Figs. 8b and 8c at 340 kOe) observed during the decomposition, even while significant amounts of ζ-Fe_2N and α-Fe still exist in the catalyst, is consistent with a nitrogen concentration gradient at the shrinking core interface between ζ-Fe_2N and α-Fe within the catalyst particle and reflects a diffusion-limited removal of nitrogen from the bulk. Note from Table 3 and the distribution curves that the total contribution of the ε-nitrides decreases from Figs. 8b to 8d, consistent with the decreasing diameter of the shell around the shrinking core of ζ-Fe_2N. At all times the thickness of the shell corresponds to 10–20% of the particle radius. With an increase of 50 to 523 K, the decomposition occurs as in Fig. 7, which was interpreted to be initially surface reaction limited. In this case, we might expect a homogeneous nitride mixture in the bulk during the much more rapid decomposition.

The Mössbauer spectra record the decomposition that occurs within the bulk. The mass spectrometric measurements reflect what is occurring at the surface during that process. Figure 7 shows a fast initial rise of ammonia in response to the introduction of hydrogen at 523 K, perhaps

TABLE 3

Room-Temperature Mössbauer Parameters for ζ-Fe_2N during Denitriding in H_2 (Fig. 8)

Spectrum	Species	I.S. (mm/s)	Q.S. (mm/s)	H (kOe)	Width (mm/s)	% area
$2\frac{1}{2}$ min H_2, Fig. 8a	ζ-Fe_2N	0.44	0.28	—	0.34	73.4
	ε-Fe_xN(dist.)	0.41	0.10	25–310	0.31	26.6
5 min H_2, Fig. 8b	ζ-Fe_2N	0.44	0.28	—	0.33	51.7
	α-Fe	−0.01	0.00	326.7	0.52	5.1
	ε-Fe_xN(dist.)	0.32	0.01	25–425	0.35	43.2
10 min H_2, Fig. 8c	ε-Fe_2N	0.44	0.27	—	0.40	23.9
	α-Fe	0.00	0.00	330.5	0.36	49.0
	ε-Fe_xN(dist.)	0.32	0.00	25–425	0.40	27.0
21 min H_2, Fig. 8d	ζ-Fe_2N	0.44	0.28	—	0.34	1.8
	α-Fe	0.00	0.00	330.5	0.34	90.0
	ε-Fe_xN(dist.)	0.26	0.01	25–310	0.31	8.2

indicating the existence of a reactive surface N-containing species that is quickly removed upon introduction of hydrogen. To examine the surface species contribution to the very early time behavior shown in Fig. 7, we exposed a freshly prepared ζ-Fe_2N nitride to Ar then D_2 at 523 K. The results are shown in Fig. 9. In this experiment, the mass spectrometer was operated at low ionizing voltage (15 eV) to prevent fragmentation of the ammonia species. Fragmentation of the partially deuterated species would result in overlaps of several different species at each mass and thus obscure and complicate the results.

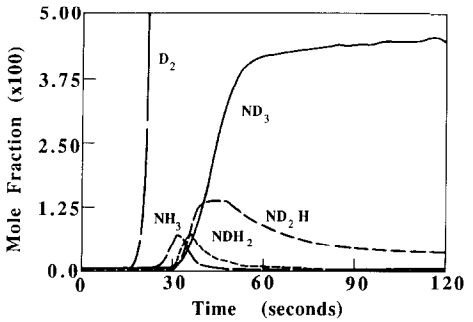

FIG. 9. Transient mass spectrometric measurement of the decomposition in D_2 of ζ-Fe_2N, nitrided in NH_3 at 673 K for 6 h, cooled to 523 K, purged in Ar, and finally exposed to D_2 at 523 K.

In order to obtain the data in Fig. 9, the catalyst was nitrided in pure ammonia at 673 K for 6 h, cooled to 523 K, and purged with argon for 5 min to remove gas-phase ammonia. NH_x species on the surface were then reacted with deuterium. The presence of NH_xD_{3-x} in the effluent shows clearly that the fresh surface retains some hydrogen. The appearance of each of the species NH_3 to ND_3 in order of increasing deuterium substitution is a result of chromatographic isotopic exchange at the leading edge of the deuterium pulse. Integration of the signals corresponding to the various hydrogen-containing species yields the total quantity of H retained by the catalyst after the argon purge; in this case, 3.5 ± 1 monolayers worth of hydrogen. One monolayer in this instance reflects the BET measurement of surface area, using the assumption of 1.2×10^{15} sites/cm^2 for Fe. Blank experiments performed under identical conditions but without the catalyst indicated that this hydrogen indeed comes from the iron catalyst. The uncertainty in the measurement is the result of the uncertainty in the calibration. Small changes

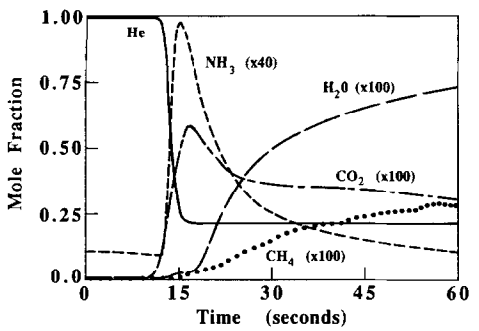

FIG. 10. Transient mass spectrometric measurement of a switch from He to 3 : 1 : 1 H_2 : CO : He at 523 K over ε-$Fe_{2.7}N$. The drop in the He curve denotes the switch in gas-phase composition.

in the calibration factor produce large changes in the integrated area. The measured value of 3.5 monolayers of surface H allows for the existence of adsorbed NH_3 on the surface, but is also consistent with excess H on and in the surface. The nitrogen-containing species are slow to desorb in inert gases, yet are removed readily in the presence of deuterium.

Nitride Stability during Fischer–Tropsch Synthesis

We have seen that some of the nitrogen in the pure nitrides is very labile. The transient mass spectrometric approach allows us to measure relative surface reactivities directly. Figure 10 shows the response of a freshly prepared and He-purged ε-$Fe_{2.7}N$ surface to synthesis gas at 523 K with an H_2/CO ratio of 3. Between one and two monolayers' worth of ammonia comes off before methane production starts, indicating that the displacement and/or reaction of surface nitrogen-containing groups is necessary before initiation of CO hydrogenation. The CO_2 curve shows that during nitrogen removal carbon is being deposited on the surface by the Boudouard CO disproportionation reaction, since no other significant carbon-containing products appear to remove surface carbon. It is possible to calculate carbon deposition by mass balance, using the fast mass spectral analysis of all products. Integration of the oxygen-containing products minus the sum of the carbon-containing products up to the first minute accounts for a surface carbon inventory of approximately one BET monolayer. Similar experiments performed by starting synthesis over reduced α-Fe show a much higher rate of carbon deposition, presumably due to the rapid formation of a bulk iron carbide. In addition, the initial rate of CO conversion to hydrocarbons is five times greater over the iron nitride than over α-Fe. The enhancement in activity is maintained over the first few hours of synthesis. This suggests that the bulk nitride effectively blocks surface carbon depletion by the competitive pathway for rapid carbon incorporation into the bulk and results in a higher initial rate of the pathway leading to formation of hydrocarbons. The long-term steady-state rate at atmospheric pressure and 3 : 1 H_2 : CO over any of the nitrides was not found to be significantly different from that over the α-Fe precursor, confirming the results of Yeh *et al.* (*5*). Since initial carbide formation affects the initial production of hydrocarbons, we speculate that this initial reaction may also influence the rate of graphitic carbon deposition or, more generally, the total surface carbon inventory during synthesis. The slight to moderate differences in selectivity and activity observed by Anderson and co-workers (*1–3*) and Yeh *et al.* (*5*) under various conditions could be a result of these changes in initial carbon deposition and the long-term carbon inventory on the surface.

Surprisingly, further decomposition of the nitride as represented by the evolution of NH_3 does not occur to a measurable extent in Fig. 10 after Fischer–Tropsch synthesis has begun. Since the nitride readily decomposes in pure hydrogen, we take this result as indicating that a carbonaceous species at the surface effectively blocks further ε-nitride decomposition in synthesis gas. When the initial nitride is ζ-Fe_2N, however, there is an initial loss of

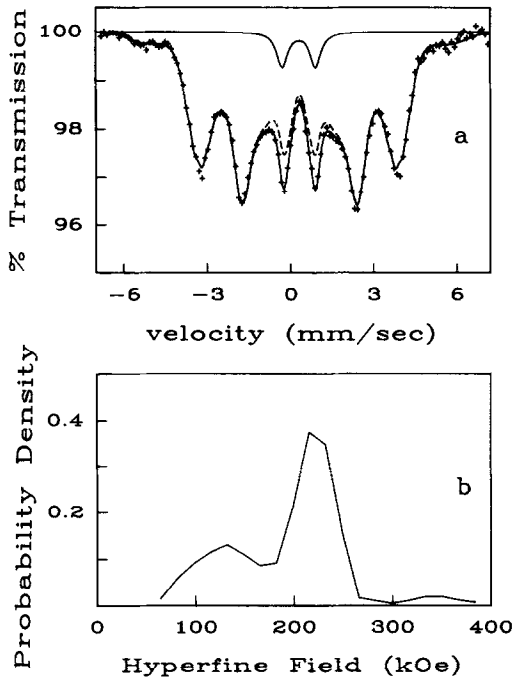

FIG. 11. Room-temperature Mössbauer data for ζ-Fe_2N nitride after 17 min reaction in 3 : 1 H_2 : CO at 523 K. (a) Constant-acceleration spectrum showing the Fe-Q and distribution subspectra; (b) hyperfine field distribution of the residual after subtraction of the Fe-Q doublet.

bulk nitrogen to convert the nitride to the ε phase. As shown below, for the ζ-nitride, the initial decomposition accounts for approximately 20% loss of bulk nitrogen over the first 17 min. Thus, the rate of nitrogen removal and/or replacement from the bulk depends on the initial concentration of bulk nitrogen, on diffusion through a rapidly formed carbon layer, and on the limited availability of surface sites for hydrogenation of surface nitrogen.

The bulk phase present after 17 min of exposure of ζ-Fe_2N to synthesis gas with an H_2/CO ratio of 3 at a temperature of 523 K is shown by the Mössbauer spectrum in Fig. 11. The fitted parameters are given in Table 4. The spectrum shows the characteristics of an ε-nitride, indicating that the ζ phase is quickly decomposed to the ε phase in synthesis gas. To accommodate the distribution of phases in this catalyst, the spectrum was fit with a distribution of hyperfine fields. Such a fit and the calculated distribution of fields are also shown in Fig. 11. The incorporation of a small amount of carbon as a carbonitride is possible as an assignment for the species at approximately 130 kOe. The ratio of 220 kOe/130 kOe for the Fe(II)/Fe(III) fields is close to that for ε-$Fe_{2.52}N$ in Fig. 3a (210/110), suggesting that the 130-kOe field is ε-III. Taking the 220-kOe field as ε-II and the 130-kOe field as ε-III yields a stoichiometry of $Fe_{2.55}N$, or a loss of 22% of the original bulk nitrogen during the first 17 min. This stoichiometry is approximately equal to the $Fe_{2.52}I$ (I = C or N) stoichiometry obtained by Chen *et al.* (*9*) after 3 h of synthesis. We note that this relatively rapid loss of bulk nitrogen was from a ζ-Fe_2N precursor, and not the ε-$Fe_{2.7}N$ catalyst used in Fig. 10. Figure 6b also indicated that this change from the ζ phase to the ε phase occurs within the first few minutes. The long-term steady-state catalyst retains a substantial fraction of the bulk nitrogen, however, as other studies have shown (*1*, *2*, *4*, *9*). Apparently, the

TABLE 4

Room-Temperature Mössbauer Parameters for ζ-Fe_2N after 17 Min of Reaction (Fig. 11)

Species	I.S. (mm/s)	Q.S. (mm/s)	H (kOe)	Width	% area
Fe-Q	0.31	1.19	—	0.47	7.5
Fe(dist.)	0.31	0.00	50–400	0.45	92.5

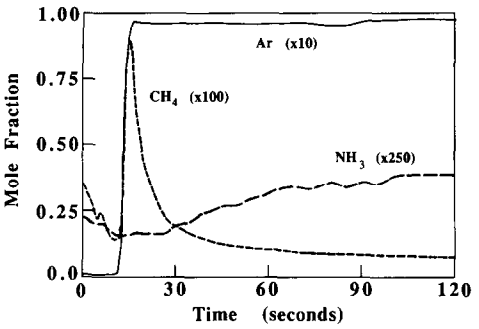

FIG. 12. Hydrogenation of ε-$Fe_{2.7}N$ after 5 min of reaction in 3 : 1 : 1 H_2 : CO : He, followed by a short pulse (10 s) of He, and then by 9 : 1 H_2 : Ar at 523 K.

denitriding that occurs in synthesis gas slows to a virtually insignificant rate during the first hour of reaction. For the ε-nitride, the blockage of decomposition occurs during the first minute.

The availability of species on the surface of the ε-nitride changes dramatically during the first minutes of reaction. Figure 12 shows the response of the reacting system after 5 min on stream, followed by a short He pulse, and finally a switch to hydrogen with 10% argon used as a time marker. The burst of methane, corresponding to 50% of a monolayer in the initial spike, is characteristic of excess reactive surface carbon (*28*). Ammonia evolves only slowly from the catalyst (note the scale). Because of the high reactivity of surface nitrogen species just demonstrated above, we take this result to indicate very low nitrogen content on the surface of the working catalyst. In addition, the continued slow rate of nitride decomposition indicates that carbon in the surface layers blocks the rapid denitriding that occurs in the pure nitride phases. Apparently, the slow hydrogenation to methane in the long-time transient of Fig. 12 is the slow removal of this graphitic/carbidic surface carbon.

CONCLUSIONS

Three of the major phases of iron nitride were synthesized in atmospheric pressure ammonia/hydrogen mixtures at different temperatures, and the phases identified by Mössbauer spectroscopy, XRD, and quantitative integration by transient mass spectrometry of ammonia evolved from the decomposition of the nitride. The room-temperature Mössbauer spectra of ε-Fe_xN ($2 < x < 3$) show a collapse of magnetic hyperfine structure as nitrogen content increases, demonstrated here by fitting these spectra with a distribution of hyperfine fields.

The decomposition of the bulk nitride in hydrogen at 523 K is rapid and is consistent with a model invoking surface reaction as the rate-limiting step initially. At 473 K, however, phases within the bulk remain intact and the decomposition of ζ-Fe_2N is consistent with a shrinking core model with N diffusing through an ε-Fe_xN gradient. The Mössbauer spectral contributions for the ε-nitrides within the decomposing bulk are best fit by a distribution of hyperfine fields, with maxima in probability density around 220 kOe (representing iron with two nitrogen nearest neighbors) and around 100 kOe (three nitrogen nearest neighbor iron).

The surface of ζ-Fe_2N has a reactive nitrogen-containing species, which does not desorb in inert atmospheres, but reacts or is displaced immediately in hydrogen or CO/H_2 mixtures. Decomposition in deuterium shows that the surface has 3.5 monolayers of hydrogen either associated with the reactive nitrogen species or on or in the surface. The partially deuterated ammonia evolved exchanges rapidly with the hydrogen-containing surface species further along the bed.

The bulk nitride is stable in helium below 600 K and loses less than 5% of the ζ phase in 2 h in pure CO at 523 K. In H_2/Co at 523 K, however, ζ-Fe_2N rapidly converts to an ε-Fe_xN phase. Nitrogen in the bulk is thereafter much more stable, exchanging with carbon slowly during synthesis.

Active surface nitrogen is not present at the surface during the Fischer–Tropsch reaction. Since the bulk nitrogen is very slow

to react with hydrogen after only 5 min of synthesis reaction, we speculate that the surface contains no iron nitride during synthesis. In addition, the activity for the prenitrided iron is similar to that of prereduced iron after long times on stream, suggesting that the active surface in both cases may be of the same carbidic nature. The initial enhancement of activity over the nitrides, probably due to the blockage of the competitive pathway to carbon incorporation into the bulk, continues for the first few hours of synthesis.

ACKNOWLEDGMENTS

We are grateful for support of this work by the National Science Foundation, Grant CBT-8519688, and by the Department of Energy, Grant DE-FG-22-82 PC50804.

REFERENCES

1. Anderson, R. B., Shultz, J. F., Seligman, B., Hall, W. K., and Storch, H. H., *J. Amer. Chem. Soc.* **72,** 3502 (1950).
2. Anderson, R. B., "Advances in Catalysis" (W. G. Frankenburg, V. I. Komarewsky, and E. K. Rideal, Eds.), Vol. 5, p. 355. Academic Press, San Diego, 1953.
3. Anderson, R. B., *Cat. Rev. Sci. Eng.* **21,** 53 (1980).
4. Yeh, E. B., Jaggi, N. K., Butt, J. B., and Schwartz, L. H., *J. Catal.* **91,** 231 (1985).
5. Yeh, E. B., Schwartz, L. H., and Butt, J. B., *J. Catal.* **91,** 241 (1985).
6. Lehrer, E., *Z. Elektrochem.* **36,** 383 (1930).
7. Jack, K. H., *Proc. R. Soc. London A* **208,** 208 (1951).
8. Bouchard, R. J., Frederick, C. G., and Johnson, V., *J. Appl. Phys.* **45,** 4067 (1974).
9. Chen, G. M., Jaggi, N. K., Butt, J. B., Yeh, E., and Schwartz, L. H., *J. Phys. Chem.* **87,** 5326 (1983).
10. Amelse, J. A., Schwartz, L. H., and Butt, J. B., *J. Catal.* **72,** 95 (1981).
11. Raupp, G. B., and Delgass, W. N., *J. Catal.* **58,** 337 (1979).
12. Niemantsverdriet, J. W., Ph.D. dissertation, Technique Hogeschool, Delft, Netherlands (1983).
13. Niemantsverdriet, J. W., van der Kraan, A. M., and Delgass, W. N., *J. Catal.* **89,** 138 (1984).
14. Hesse, J., and Rübartsch, *J. Phys. E* **7,** 497 (1974).
15. Wivel, C., and Morup, S., *J. Phys. E* **14,** 513 (1981).
16. Clauser, M. J., *Solid State Commun.* **8,** 781 (1970).
17. Nozik, A. J., Wood, J. C., and Haacke, G., *Solid State Commun.* **7,** 1677 (1969).
18. Wood, J. C., and Nozik, A. J., *Phys. Rev. B.* **4,** 2224 (1971).
19. Gatte, R. R., and Phillips, J., *J. Phys. Chem.* **91,** 5961 (1987).
20. Wickmann, H. H., *in* "Mössbauer Effect Methodology" (I. J. Gruverman, Ed.), Vol. 2, p. 39. Plenum, New York, 1966.
21. Morup, S., Dumesic, J. A., and Topsoe, H., *in* "Applications of Mössbauer Spectroscopy" (R. L. Cohen, Ed.), Vol. II, p. 1. Academic Press, San Diego, 1980.
22. Foct, J., and Rochegude, P. *Hyperfine Interact.* **28,** 1075 (1986).
23. Foct, J., LeCaer, G., Dubois, J. M., and Faivre, R., "International Conf. on Carbides, Borides and Nitrides in Steel, Kolobrzeg, Poland," p. 225. 1978.
24. Lin, S. C., and Phillips, J., *J. Appl. Phys.* **58,** 1943 (1985).
25. Bainbridge, J., Channing, D. A., Whitlow, W. H., and Pendlebury, R. E., *J. Phys. Chem. Solids* **34,** 1579 (1973).
26. Ertl, G., Huber, M., and Thiele, N., *Z. Naturforsch. A* **34,** 30 (1979).
27. Emmett, P. H., and Love, K. S., *J. Phys. Chem.* **55,** 4043 (1933).
28. Bianchi, D., Tau, L. M., Borcar, S., and Bennett, C. O., *J. Catal.* **84,** 358 (1983).